Electronic Supplementary Material (ESI) for Physical Chemistry Chemical Physics.
This journal is © the Owner Societies 2020

Use of scavenger agents in heterogeneous photocatalysis: truths, half-truths, and misinterpretations

Jéssica Tamara Schneider, Daniele Scheres Firak*, Ronny Rocha Ribeiro, Patricio Peralta-Zamora

Departamento de Química, Universidade Federal do Paraná, C.P. 19032, CEP 81531-980, Curitiba, Brazil

1 – Experimental conditions

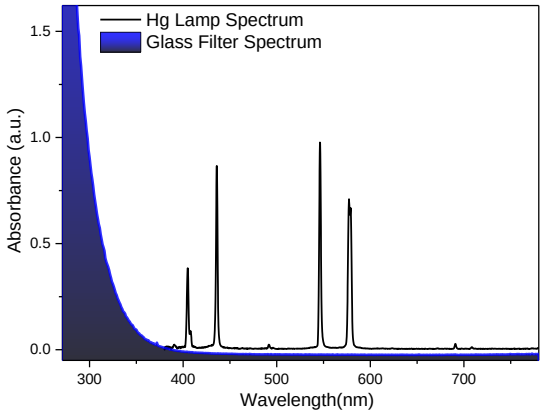

Figure S1- Hg vapor lamp spectra (acquired in EVERFINE high accuracy array spectroradiometer, model HAAS 2000) and cut-off of the glass filter used during photodegradation experiments (acquired in a Varian spectrometer, model Cary 50 Bio)

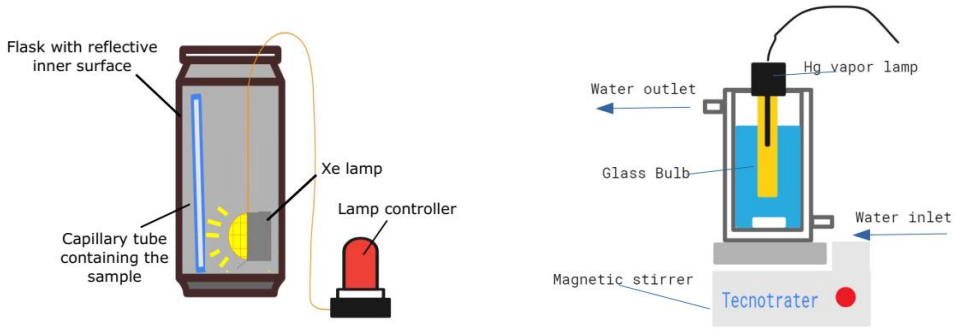

Figure S2- Schematic drawing of experiments conducted during EPR studies (on the left) and phenol degradation (on the right)

2- Chromatographic conditions:

Phenol degradation was evaluated via High-Performance Liquid Chromatography (HPLC, Varian LC-920), with a UV detector (DAD), using a C18 reverse-phase column (Microsorb, 250 mm x 4.6 mm, particle size of 5 µm) at 30 ºC, with a sample injection of 50 µL. A gradient of acetonitrile (J.T. Baker, 99.98 %)/water (Milli-Q®, 18.2 mΩ cm, Millipore-Simplicity UV) was used as mobile phase. The gradient program started at 15 % acetonitrile, progressed to 100 % acetonitrile over 10 minutes, and remained in this condition for 5 minutes [1].

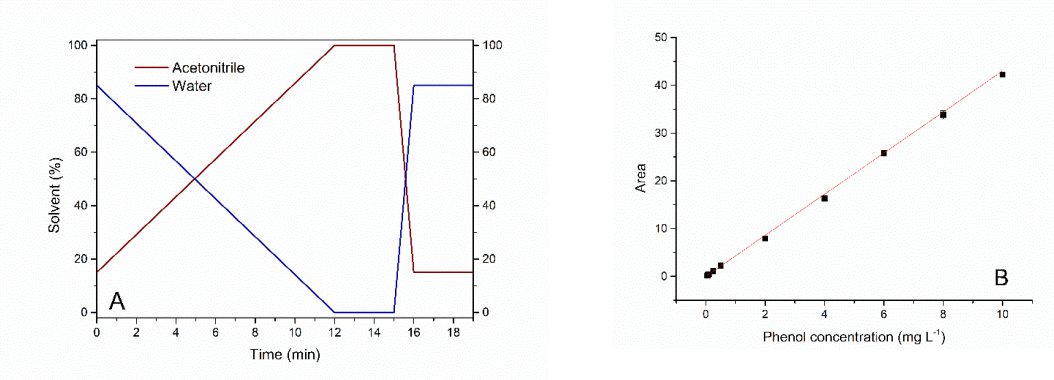

Figure S3. Gradient applied in the phenol analysis (A) and phenol analytical curve (B)

3 - Kinetic concerns:

The concentration vs. time profile was plotted using the linearized form of the first-order equation written as:

$$\ln\left(\frac{C_0}{C_t}\right) = k.t$$

Where C_0 is the initial concentration, C_t the concentration at time t, and k the rate constant corresponding the slope of the lines represented in Figure S4. As one can see in this figure, the profile does not behave as a continuous straight line. In fact, two or more regions with a linear behavior can be seen; a sharp increase develops in the first 10 minutes for most reactions, and a slower increase takes place after 10 minutes, which indicates the process cannot be described by exclusively one rate constant. More specifically, there are more than one step in the reaction mechanism controlling the velocity rate at different reaction times.

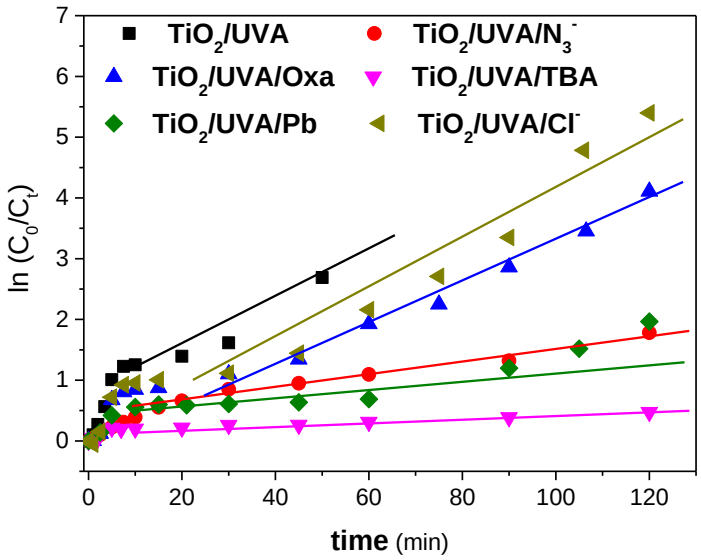

Figure S4. First-order plot for scavengers and interfering species in TiO_2/hv

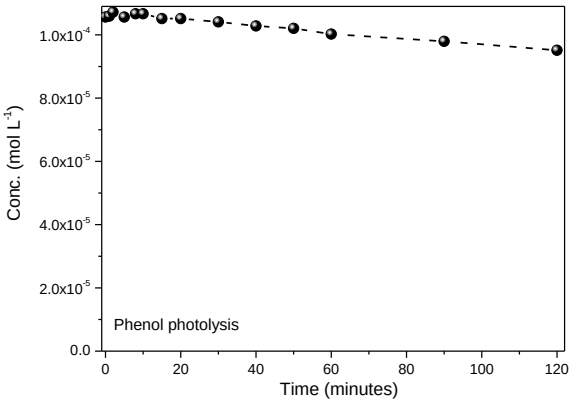

Figure S5 – Control reaction of phenol photolysis. Irradiation is provided by a high-pressure Hg vapor lamp. Initial phenol concentration 1 10^{-4} mol L^{-1}

4- Simulated EPR Spectrum:

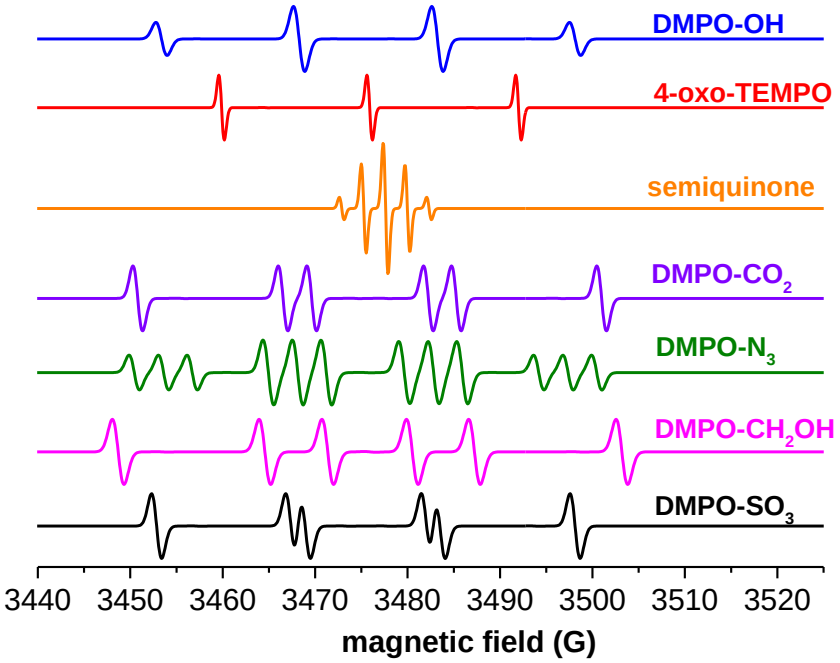

Figure. S6. Simulated EPR spectrum of all adducts and organic radicals observed in this work

5- Controls:

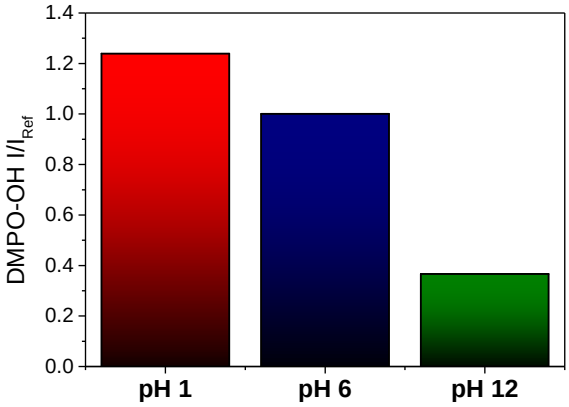

Figure. S7. Relative intensity of DMPO-OH signals in photocatalysis experiments conducted at pH 1, 6, and 12. TiO_2 and DMPO-OH concentrations were of 250 mg L^{-1} and 50 mmol L^{-1}, respectively – the same used in phenol photocatalytic degradation. pH was adjusted using solutions of 25 mmol L^{-1} of NaOH or H_2SO_4

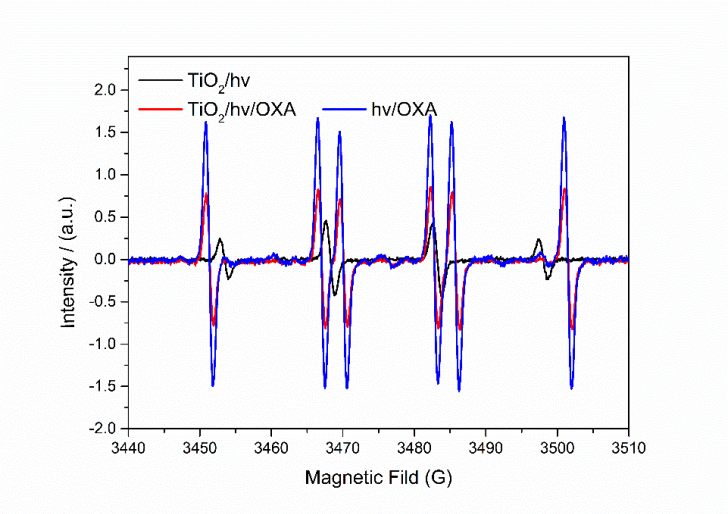

Figure. S8: EPR experiments conducted in the presence of oxalate with DMPO irradiated with a Xenon lamp in the presence (red line) and absence (blue line) of TiO_2

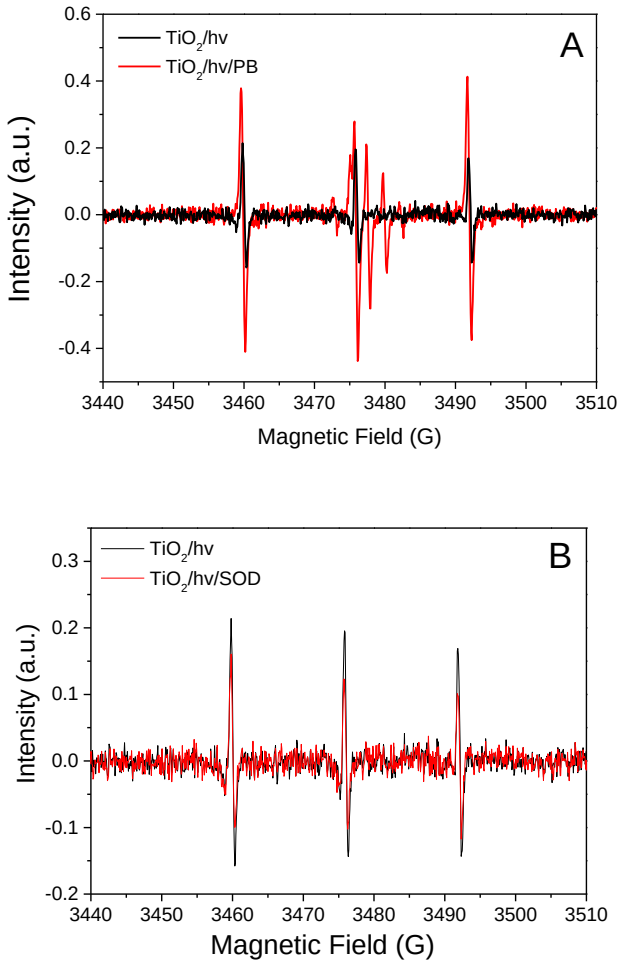

Figure. S9: TiO_2/hv EPR experiments conducted in the presence of (A) p-benzoquinone (pB) and (B) SOD with the spin trapping agent TEMP irradiated with a Xenon lamp

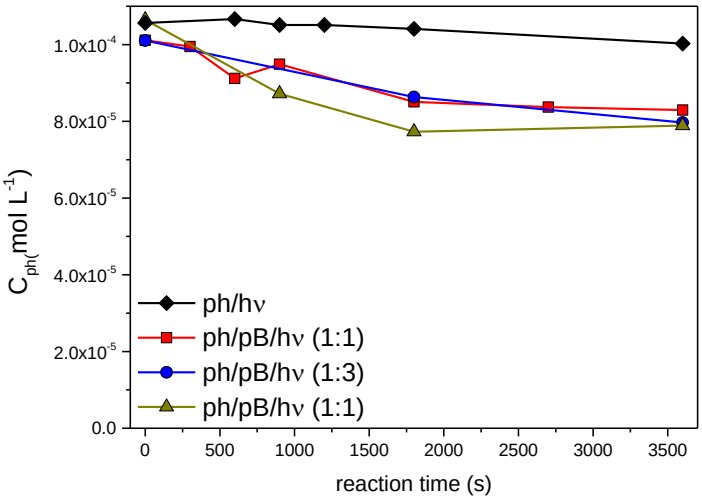

Figure S10: Experiments conducted in the presence of p-benzoquinone (pB), phenol (ph), and radiation (mercury-vapor lamp) in a 200 mL reactor. The black line represents the reference experiment (ph/UVA, i.e., the photolysis of phenol) conducted with 20 µmol of ph. The red line is the experiment conducted in the presence of ph and pB using 20 µmol of pB and ph. The blue line represents the experiment using 20 µmol of ph and 60 µmol of pB. The green line represents the experiment conducted using 2 mmol of pB and ph. Solid lines are only to guide eyes. All experiments were diluted previously to the analysis to 0.1 mmol L^{-1}

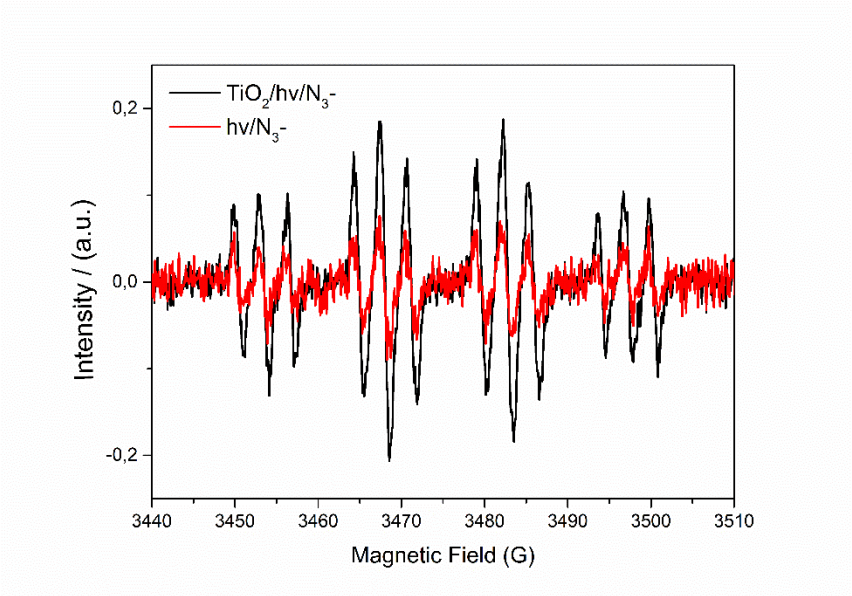

Figure. S11: EPR experiments conducted in the presence of TiO_2/hv/azide and azide/hy with DMPO irradiated with a Xenon lamp

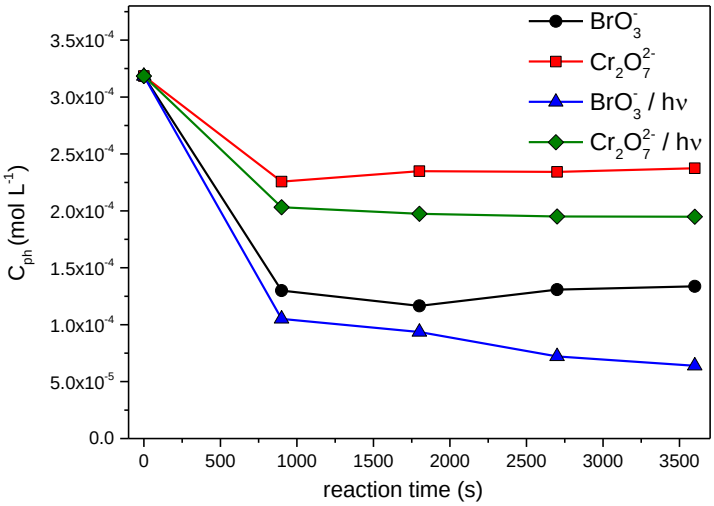

Figure S12: Experiments of phenol (300 µmol L^{-1}) degradation conducted in the presence of dichromate and bromate (6 mmol L^{-1}), with and without radiation incidence. The black and the blue lines represent the experiments conducted in the presence of bromate (BrO_3^-), in the absence and presence of radiation (UVA), respectively. The red and the green lines represent the experiments conducted in the presence of dichromate ($Cr_2O_7^{2-}$), in the absence and presence of radiation (UVA), respectively. Solid lines are to guide eye

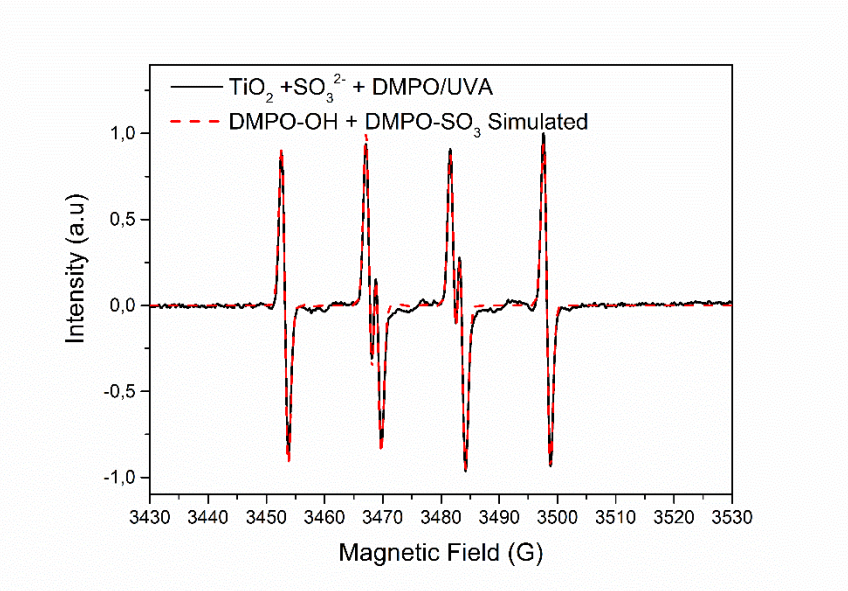

Figure S13. DMPO-OH and DMPO-SO_3 overlapped signals. 90 % of DMPO-SO_3 and 10 % of DMPO-OH contribution, according to the simulation

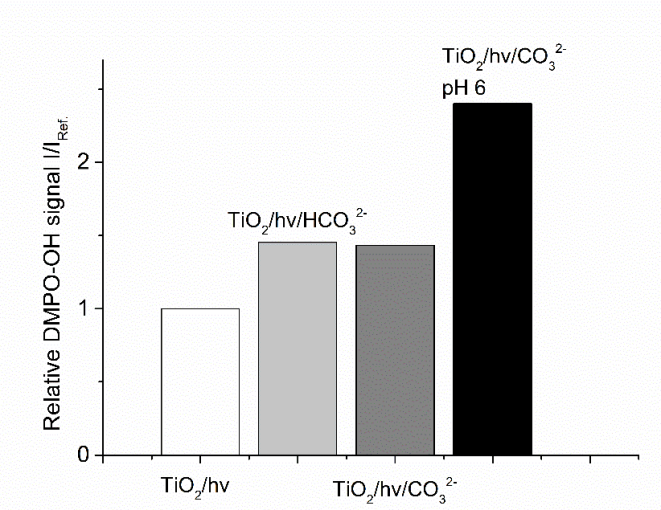

Figure S14. Effect of bicarbonate and carbonate in the DMPO-OH signal

Table S1: Redox potential of the substances described in the manuscript relative to the standard hydrogen electrode (SHE)

ROS		Ref.
$O_2 + e^- \rightarrow O_2^{\cdot -}$	$E^0 = -0.33\ V$	[2]
$O_2 + e^- + H^+ \rightarrow HO_2^{\cdot}$	$E^0 = -0.46\ V$	[2]
$O_2^{\cdot -} + e^- + 2H^+ \rightarrow H_2O_2$	$E^0 = +0.94\ V$	[2]
$H_2O_2 + e^- + H^+ \rightarrow HO^{\cdot} + H_2O$	$E^0 = +0.32\ V$	[2]
$HO^{\cdot} + e^- + H^+ \rightarrow H_2O$	$E^0 = +2.33\ V$	[2]
$HO_2^{\cdot} + e^- + H^+ \rightarrow H_2O_2$	$E^0 = +1.06\ V$	[2]
$^1O_2 + e^- \rightarrow O_2^{\cdot -}$	$E^0 = +0.65\ V$	[2]
$H_2O_2 + 2e^- + 2H^+ \leftrightarrow 2H_2O$	$E^0 = +1.77\ V$	[3]
Photocatalysis reactions		
$TiO^- + e^- \rightarrow TiOH$	$E^0_{red} = +2.53\ V$	[4]
$Ti^{4+} + e^- \rightarrow Ti^{3+}$	$E^0_{red} = -0.52\ V$	[4]
Scavenging Species		
$I_{2\,(s)} + 2e^- \leftrightarrow 2\ I^-$	$E^0 = +0.53\ V$	[3]
$I_2^{\cdot -} + e^- \rightarrow 2\ I^-$	$E^0 = +1.03\ V$	[5]
$I_3^- + 2e^- \leftrightarrow 3\ I^-$	$E^0 = +0.54\ V$	[3]
$Cl_{2\,(g)} + 2e^- \leftrightarrow 2\ Cl^-$	$E^0 = +1.36\ V$	[3]
$Cl_2^{\cdot -} + e^- \rightarrow 2\ Cl^-$	$E^0 = +2.09\ V$	[5]
$Cr_2O_7^{2-} + 14H^+ + 6e^- \leftrightarrow 2Cr^{3+} + 7\ H_2O$	$E^0 = +1.36\ V$	[3]
$BrO_3^- + 6\ H^+ + 6e^- \leftrightarrow Br^- + 3H_2O$	$E^0 = +1.42\ V$	[3]
$p - Q + e^- \rightarrow Q^{\cdot -}$	$E^0 = +0.29\ V$	[6]
$CO_2^{\cdot -} + e^- \rightarrow CO_2$	$E^0 = -2.0\ V$	[5]
$N_3^{\cdot} + e^- \rightarrow N_3^-$	$E^0 = +1.3\ V$	[5]
$SO_3^{\cdot -} + e^- \rightarrow SO_3^{2-}$	$E^0 = +0.63\ V$	[5]
$BrO_2^{\cdot} + e^- \rightarrow BrO_2^-$	$E^0 = +1.33\ V$	[5]
$CO_3^{\cdot -} + e^- \rightarrow CO_3^{2-}$	$E^0 = +1.50\ V$	[7]
$CO_3^{\cdot -} + e^- + H^+ \rightarrow HCO_3^-$	$E^0 = +1.78\ V$	[8]

MATLAB SIMULATION SCRIPT

```
[Data.X, Data.Y] = textread('C:\AddPathHere\AddTxtFileHere.txt',' %f %f');
Data.X = Data.X';
Data.Y = Data.Y'/max(Data.Y);

% Experimental settings

n = 2048; % Number of lines in the experimental spectra
Exp.nPoints = n;

% Spin Hamiltonian Parameters for species A and B (considering 2 species in
the same spectra)

%Species A - Example DMPO-N3
Sys.g = 2.0066; % g-factor
Sys.lwpp = [0.112 0]; % Line width provided in mT [Gauss Lorentz]
Sys.Nucs = 'H, N, N'; % Nuclei presented in hyperfine coupling interaction
fH1 = 41.1967;Sys.g ; % Hyperfine parameter from nucleus 1 given in mHz
fN1 = 41.1967;Sys.g ; % Hyperfine parameter from nucleus 2 given in mHz
fN2 = 8.4075;Sys.g; % % Hyperfine parameter from nucleus 3 given in mHz
Sys.A = [fH1; fN1; fN2]; % Hyperfine tensor
Sys.weight= 2; % Contribution in the spectra

%Species B - Example DMPO-OH
Sys2.g = 2.0066; % g-factor
Sys2.lwpp = [0.111 0]; % Line width provided in mT [Gauss Lorentz]
Sys2.Nucs = 'N, H'; % Nuclei presented in hyperfine coupling interaction
fH2 = 42.0374;Sys2.g; Hyperfine parameter from nucleus 1 given in mHz
fN3 = 42.0374;Sys2.g; Hyperfine parameter from nucleus 2 given in mHz
Sys2.A = [fH2;fN3]; % Hyperfine tensor
Sys2.weight = 1; % Contribution in the spectra

%Simulation
Data.sim = garlic({Sys,Sys2},Exp);
Data.sim = Data.sim/max(Data.sim);
Chi = sqrt(mean((Data.Y - Data.sim).^2))


% Spectra graph
plot(Data.X,Data.Y,'black',Data.X,Data.sim,'red');
xlim([Data.X(1) Data.X(n)]);
ylim([-1.1 1.1]);
legend('Experimental','Simulated');
xlabel('magnetic field [G]');

% Output
spec1 = [Data.X;Data.Y;Data.sim];
spec = fopen('C:\AddPathHere\AddNewTxtFileHere.txt','w');
fprintf(spec,'%E %E %E \n',spec1);
fclose(spec);
```

References

1 S. Stets, B. do Amaral, L. Bach, N. Nagata and P. G. Peralta-Zamora, *Environ. Sci. Pollut. Res.*, 2017, **24**, 6040–6046.

2 K. Krumova and G. Cosa, in *Singlet Oxygen: Applications in Biosciences and Nanosciences.*, 2016, pp. 5–18.

3 P. Vanýsek, in *CRC Handbook of Chemistry and Physics*, ed. D. R. Lide, CRC Press, 84th ed., pp. 8-21−8-31.

4 A. Fujishima, T. N. Rao and D. A. Tryk, *J. Photochem. Photobiol. C Photochem. Rev.*, 2000, **1**, 1–21.

5 P. Neta, R. E. Huie and A. B. Ross, *J. Phys. Chem. Ref. Data*, 1988, **17**, 1027–1284.

6 K. B. Patel and R. L. Willson, *J Chem Soc Faraday Trans I*, 1973, **69**, 814–825.

7 R. E. Huie, C. L. Clifton and P. Neta, *Radiat. Phys. Chem.*, 1991, **38**, 477–481.

8 O. Augusto and S. Miyamoto, in *Principles of Free Radical Biomedicine*, eds. K. Pantopoulos and H. M. Schipper, Nova Science Publishers, Inc., 2011, vol. 1, pp. 1–23.